Late-Stage Microsomal Oxidation Reduces Drug–Drug Interaction and Identifies Phosphodiesterase 2A Inhibitor PF-06815189

ACS Med. Chem. Lett. 2018, 9, 68−72

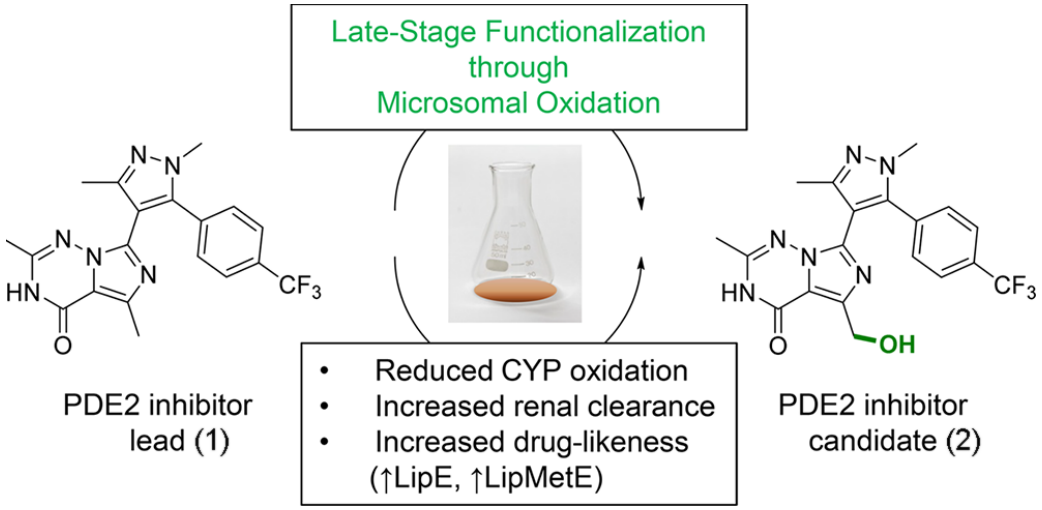

Shikha Singh Chauhan

Wipf Group Current literature

February 17th 2018

LATE STAGE C-H FUNCTIONALIZATION IN DRUG DISCOVERY

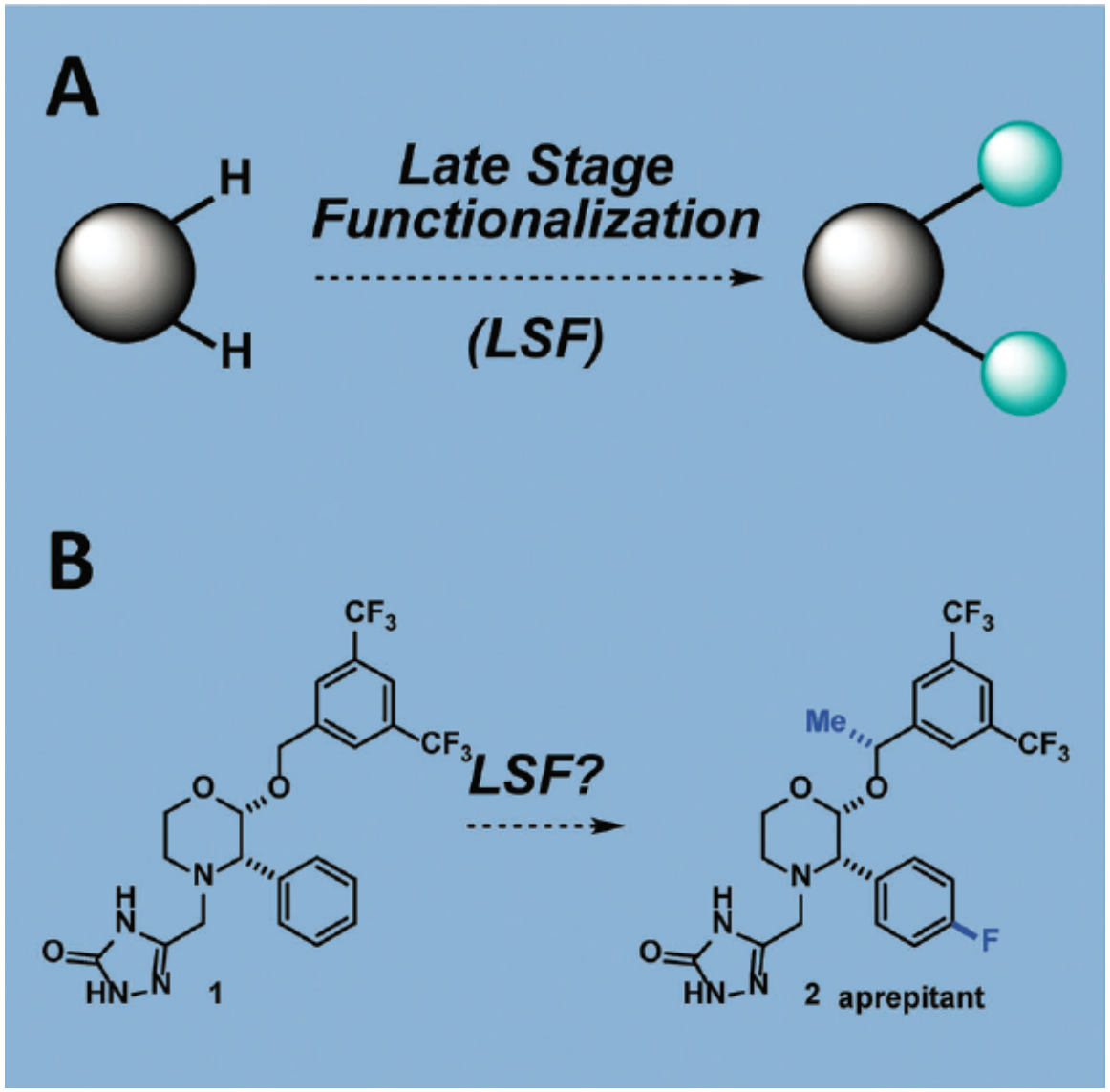

Cernak et. al., *Chem. Soc. Rev.*, 2016, 45, 546--576

DRUG-DRUG INTERACTIONS

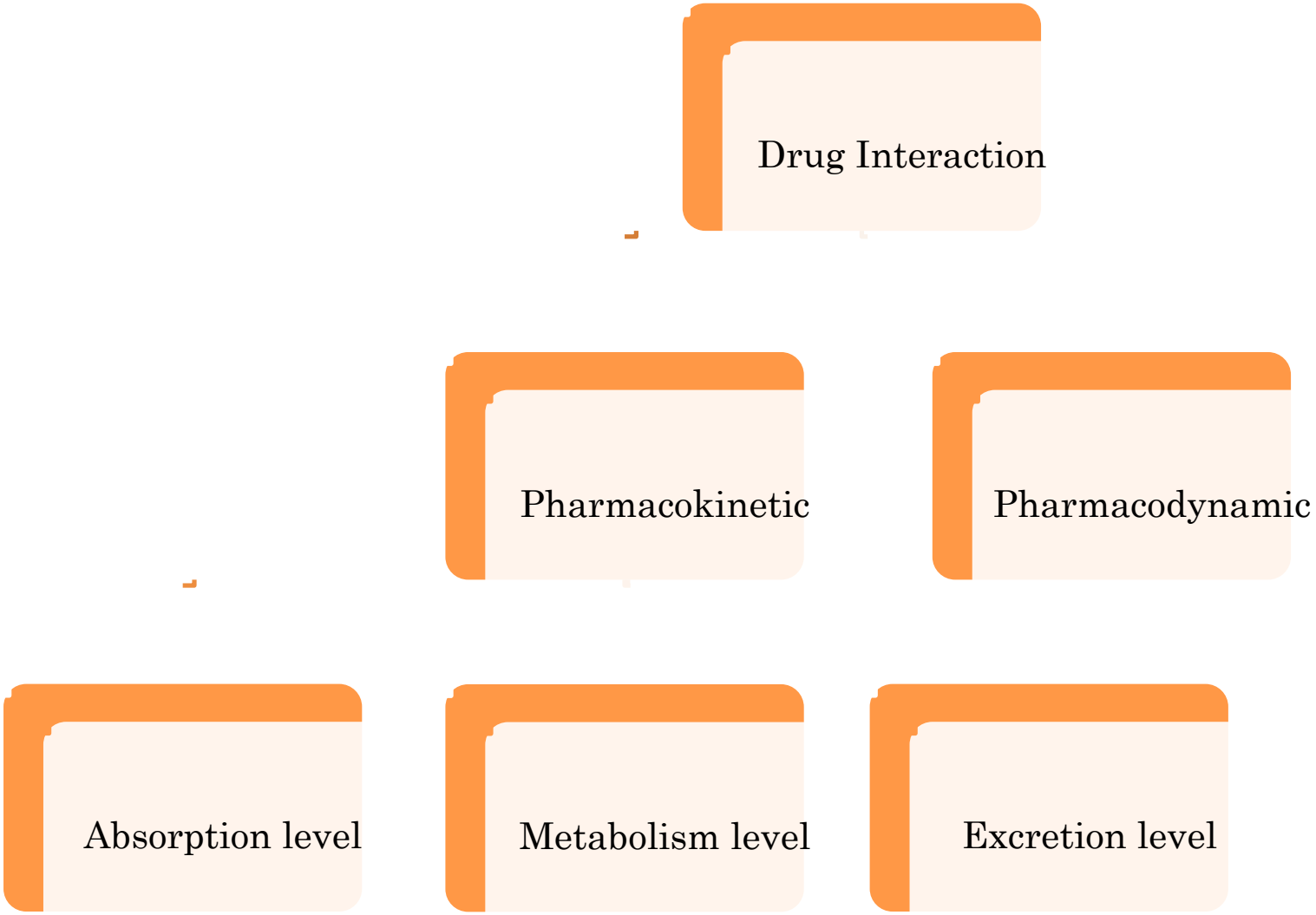

Late-Stage Lead Diversification Microsomal Screen

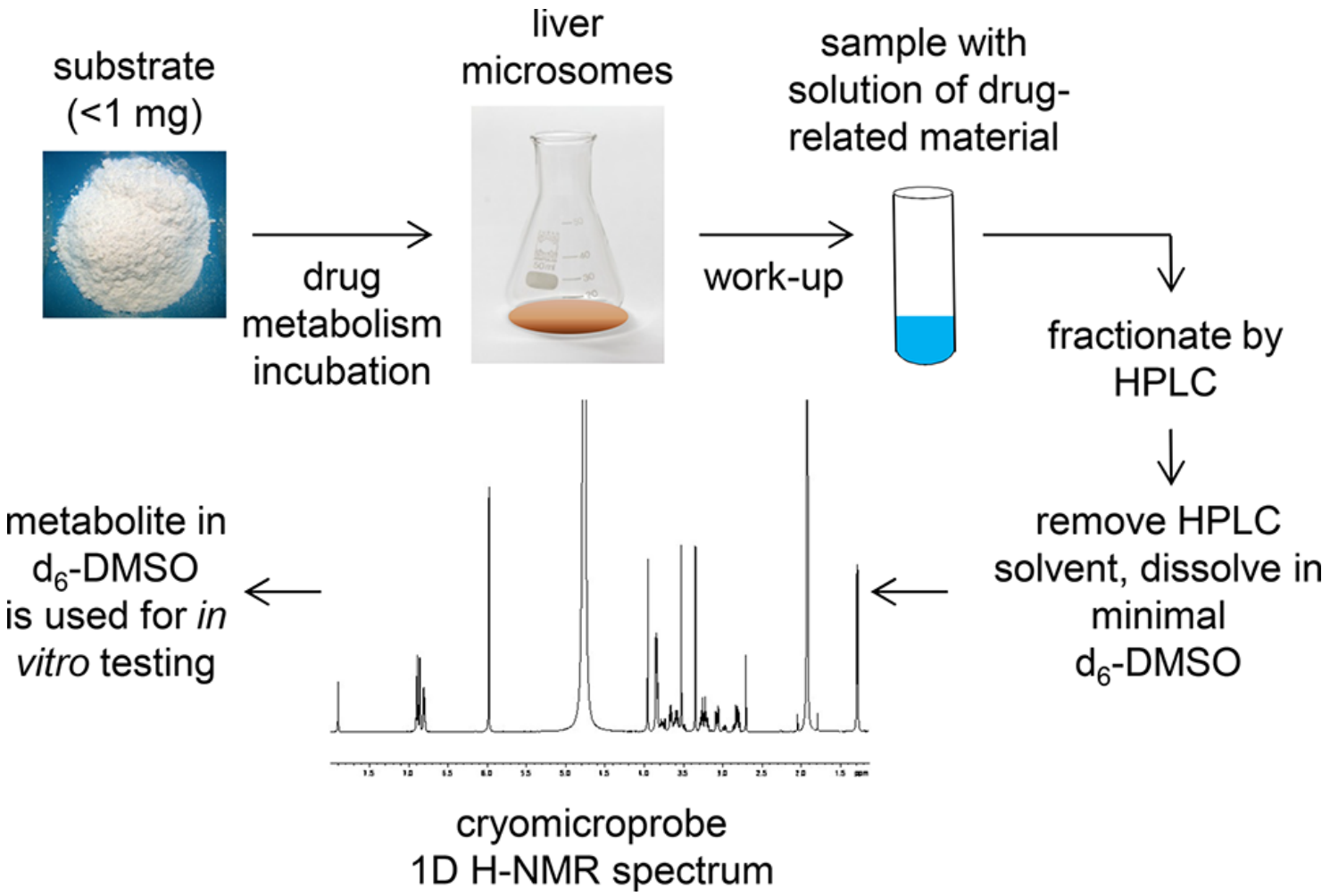

Stepan et. al., *ACS Med. Chem. Lett.* 2018, 9, 68−72

Biosynthesis of Fluorinated Analogs of Drugs Using Human Cytochrome P450 EnzymesFollowed by Deoxyfluorination

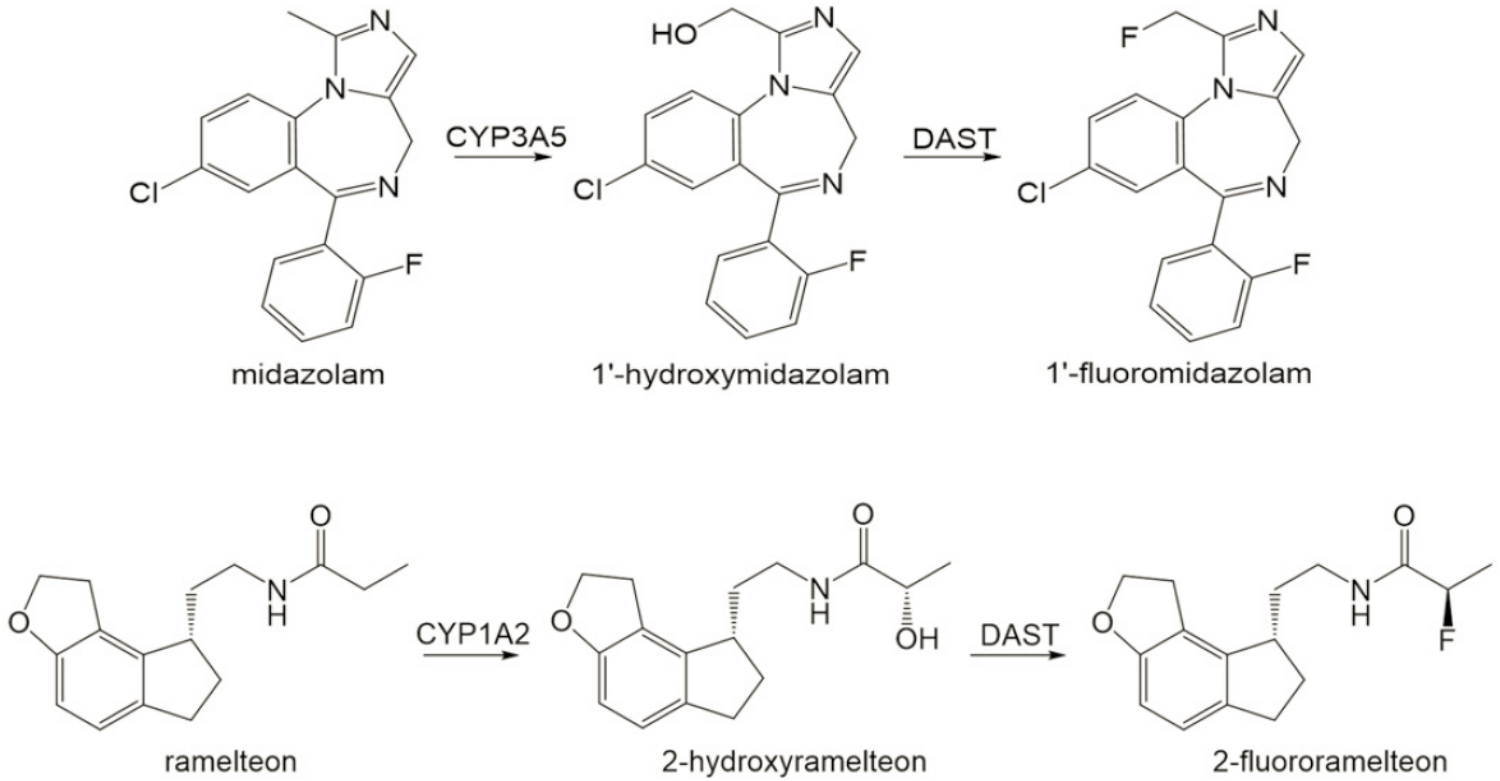

Obach et. al., Drug Metab Dispos 44:634–646

Biosynthesis of Fluorinated Analogs Contd.

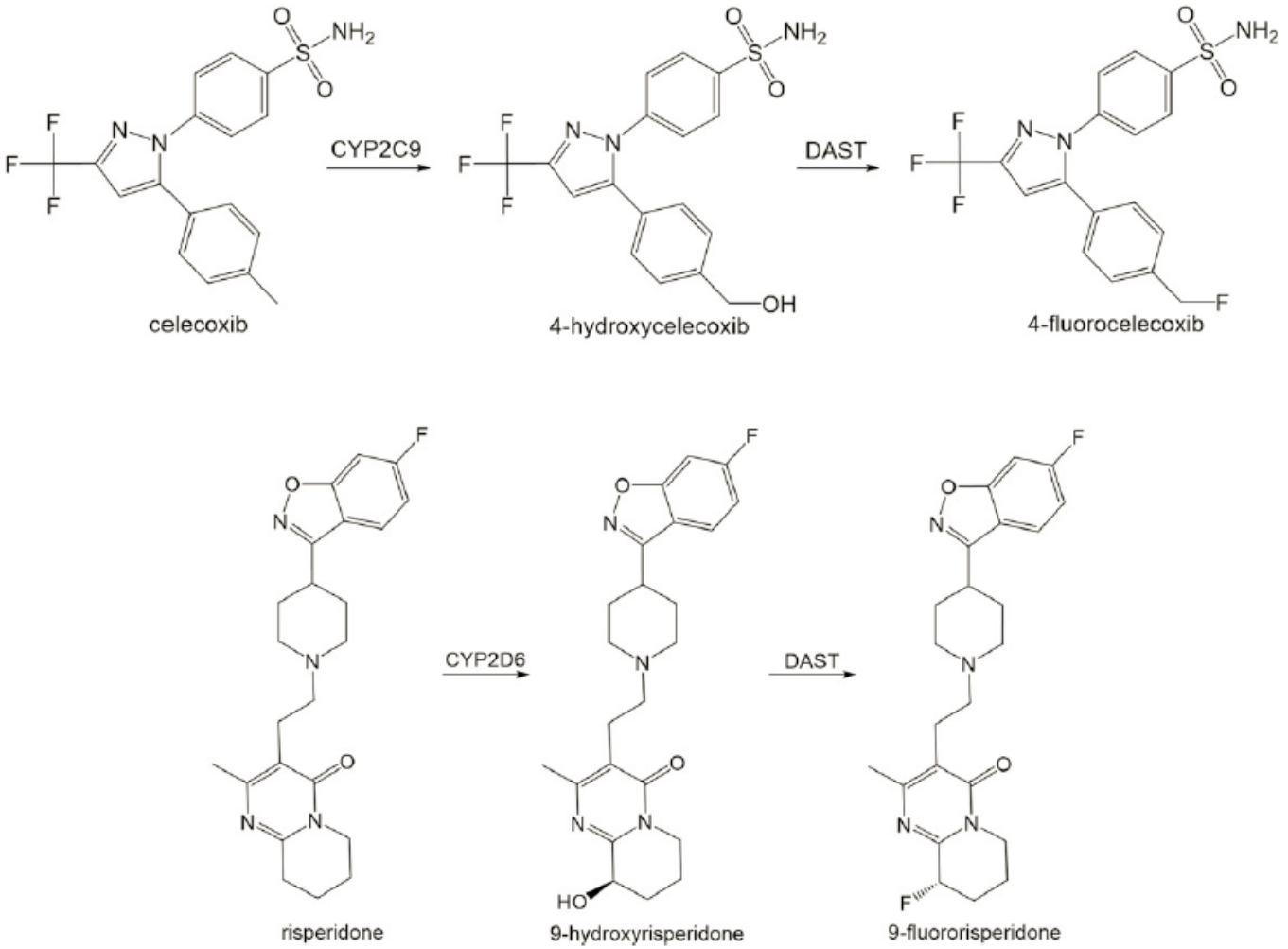

Obach et. al., Drug Metab Dispos 44:634–646

METABOLIC STABILITY

Comparison of metabolic lability in recombinant human P450 enzymes between drugs and their fluorinated analogs

Compound	Enzyme	CL_{int} (μl/min per picomole P450)		
		Parent Drug	Fluorinated Analog	Stability Factor
Midazolam	CYP3A4	23.4 (0.7)	17.7 (0.7)	1.3
Midazolam	CYP3A5	45.9 (1.0)	15.3 (0.5)	3.0
Ramelteon	CYP1A2	27.3 (6.4)	28.8 (5.1)	0.95
Celecoxib	CYP2C9	3.0 (0.4)	0.78 (0.15)	3.8
Risperidone	CYP2D6	5.6 (0.3)	0.34 (0.37)	16

Values in parentheses are standard errors.

Obach et. al., Drug Metab Dispos 44:634–646

PHOSPHODIESTERASES (PDEs)

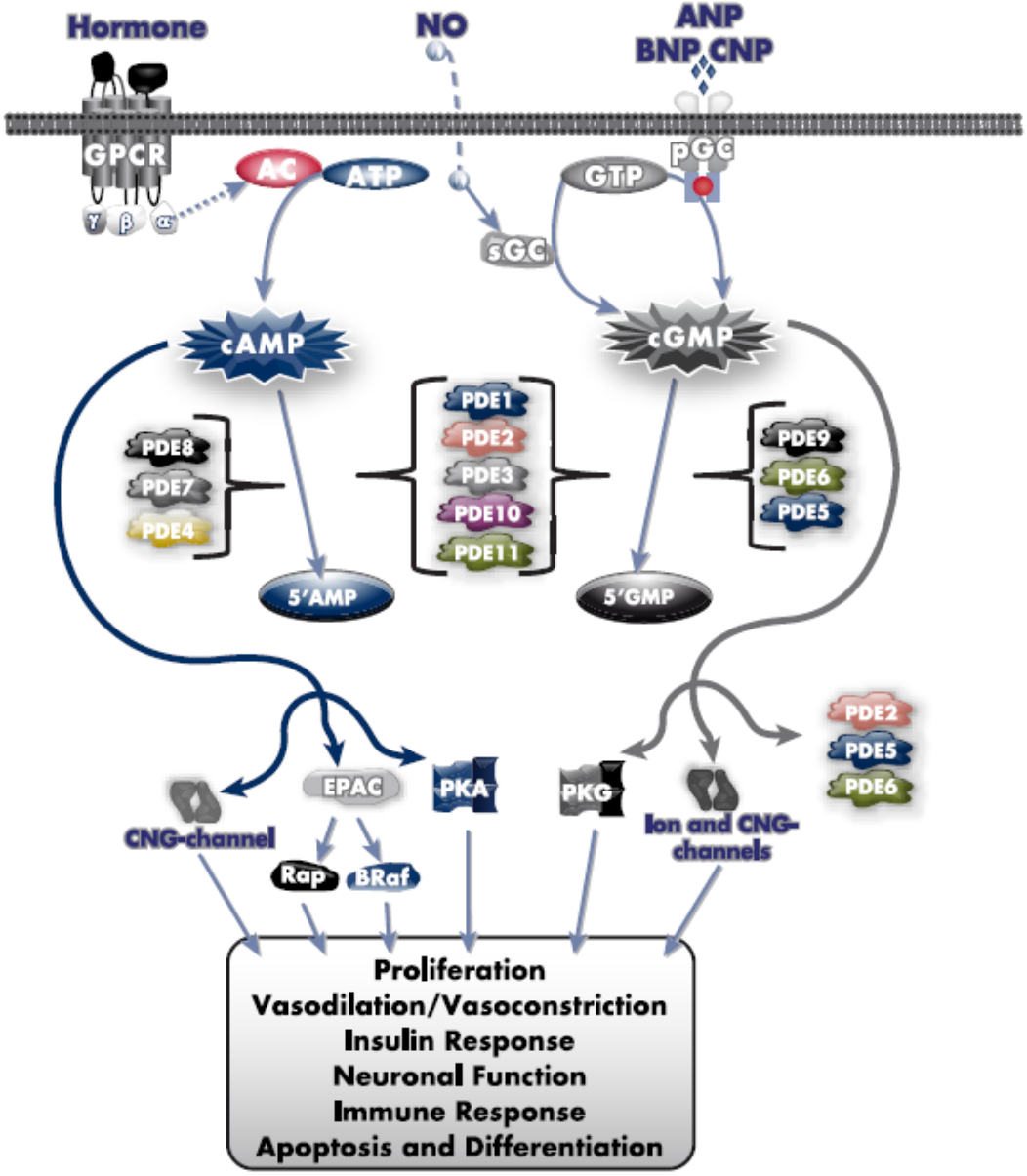

Azevedo et. al., *Endocrine Reviews*, 2014, 35(2):195–233

Design Strategy to PDE2 Inhibitor 1

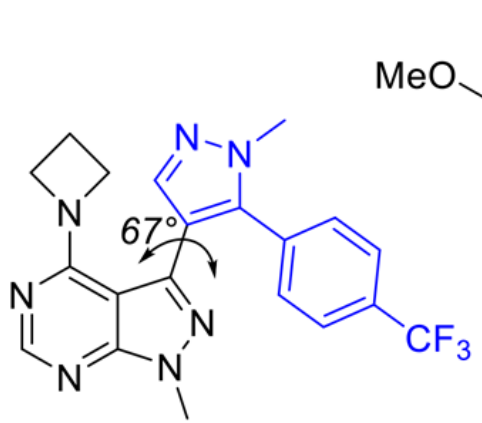

3

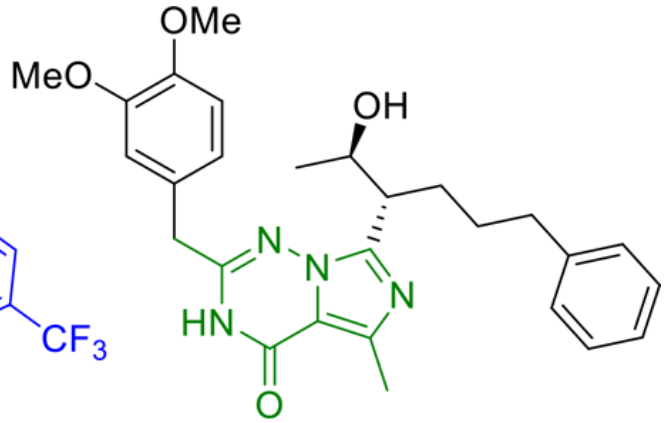

4 (BAY 60-7550)

	3	**4** (BAY 60-7550)
clogP/TPSA[a]	2.6/65	2.4/102
PDE2 IC_{50} (nM)[b]	1.6 (14)	0.2 (7)
HLM $CL_{int,s}$ (mL/min/kg)[c]	85	216
RRCK P_{app}(× 10^{-6} cm/s)[d]	22	24

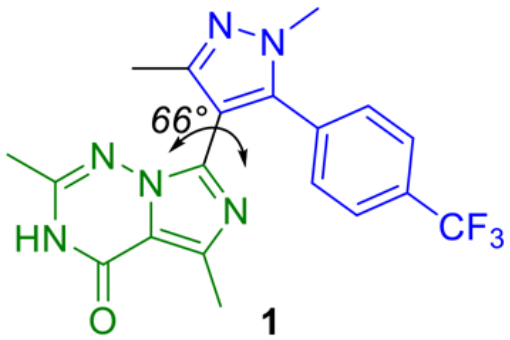

1

	1
clogP/TPSA[a]	3.3/81
PDE2 IC_{50} (nM)[b]	0.6 (6)
HLM/HHEP $CL_{int,s}$ (mL/min/kg)[c]	16/18
RRCK P_{app} (× 10^{-6} cm/s)[d]	23

Stepan et. al., *ACS Med. Chem. Lett.* 2018, 9, 68−72

MOLECULAR DOCKING

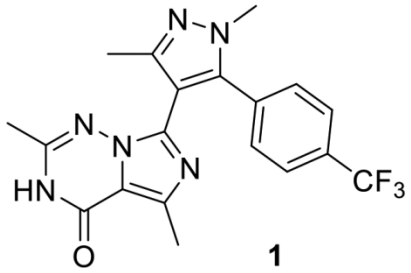

1

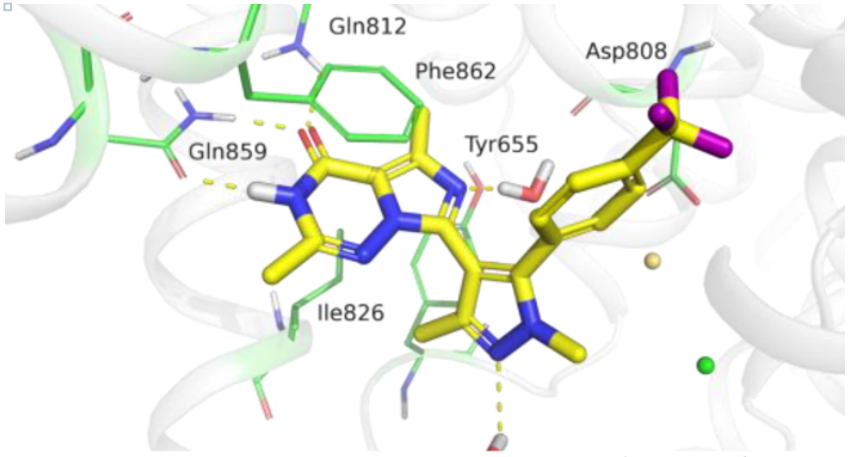

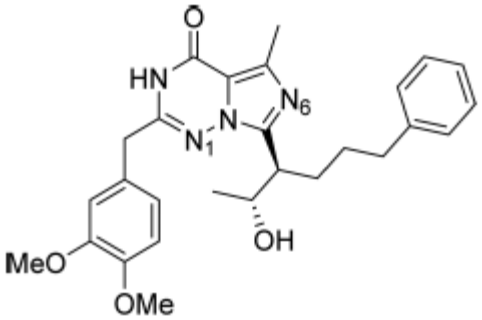

BAY 60-7550

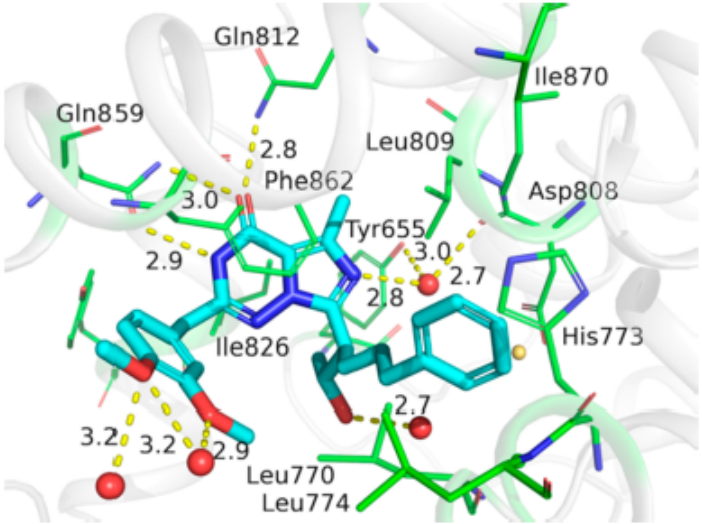

Stepan et. al., *ACS Med. Chem. Lett.* 2018, 9, 68−72

Helal, *J. Med. Chem.* 2017, 60, 5673−5698

Zhu et. Al., *J. Am. Chem. Soc.* 2013, 135, 11708−11711

DIHEDRAL ANGLE CALCULATION FOR 1

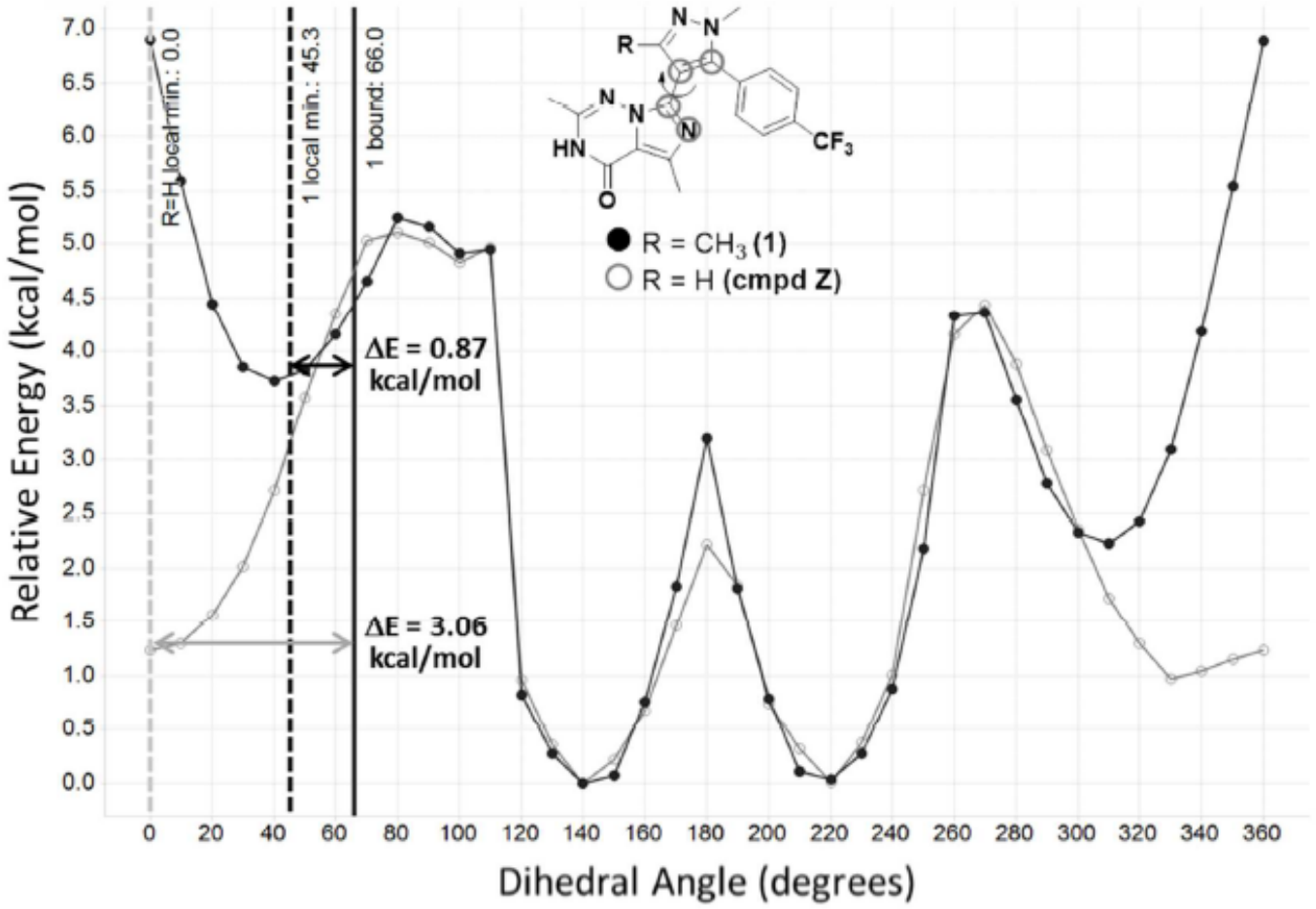

Figure S-1. **Relative energies from dihedral scan with 1 and its des-methyl analog cmpd Z.**

Stepan et. al., *ACS Med. Chem. Lett.* 2018, 9, 68−72

UHPLC-UV Chromatograms of Compound 1 Incubation Extracts from Expressed Human P450 Enzymes

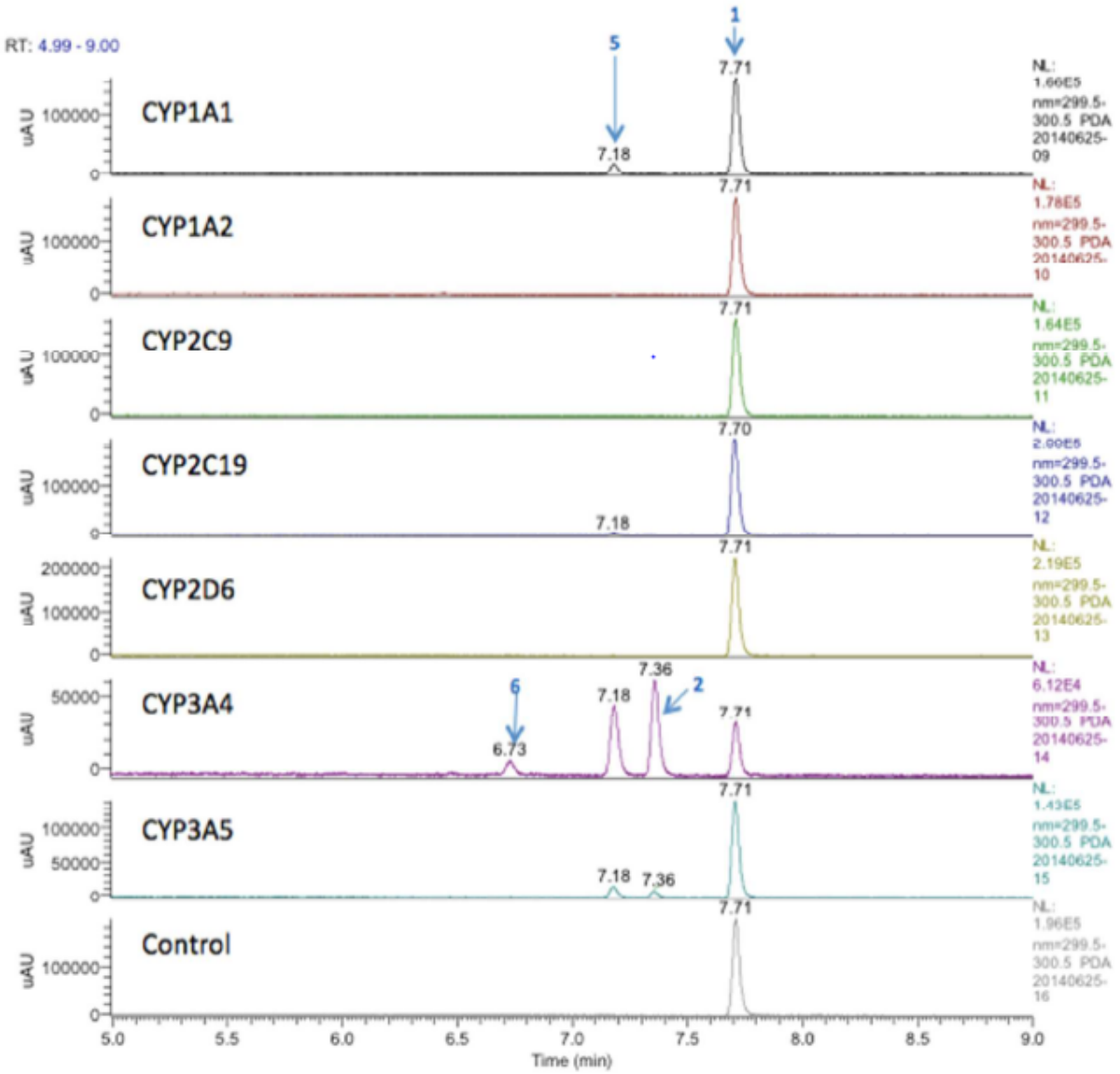

Stepan et. al., *ACS Med. Chem. Lett.* 2018, 9, 68−72

UHPLC-UV Chromatograms of Compound 1 Incubation Extracts from Liver Microsomes of various species

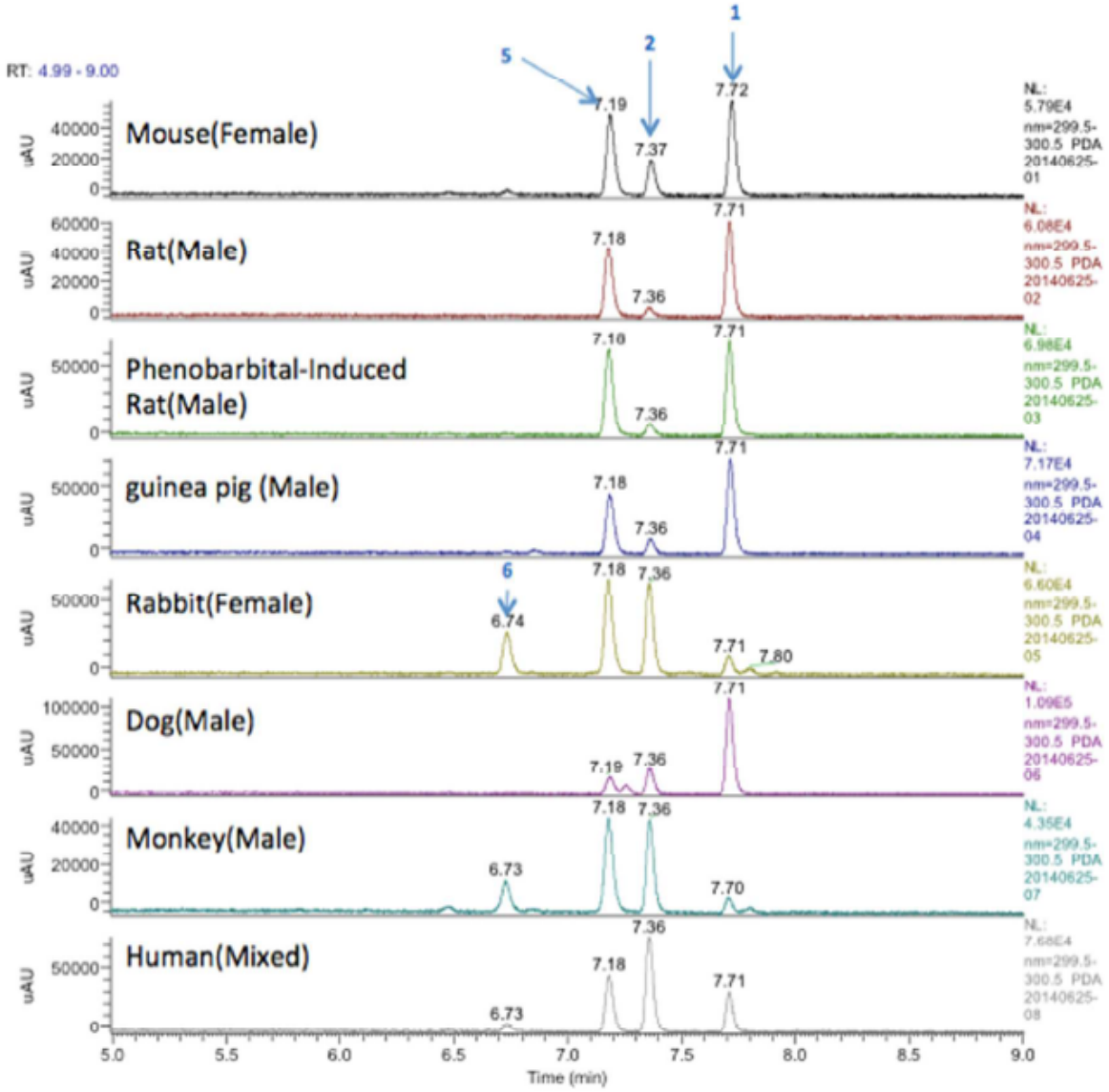

Stepan et. al., *ACS Med. Chem. Lett.* 2018, 9, 68−72

METABOLISM OF 1 IN MONKEY LIVER MICROSOMES

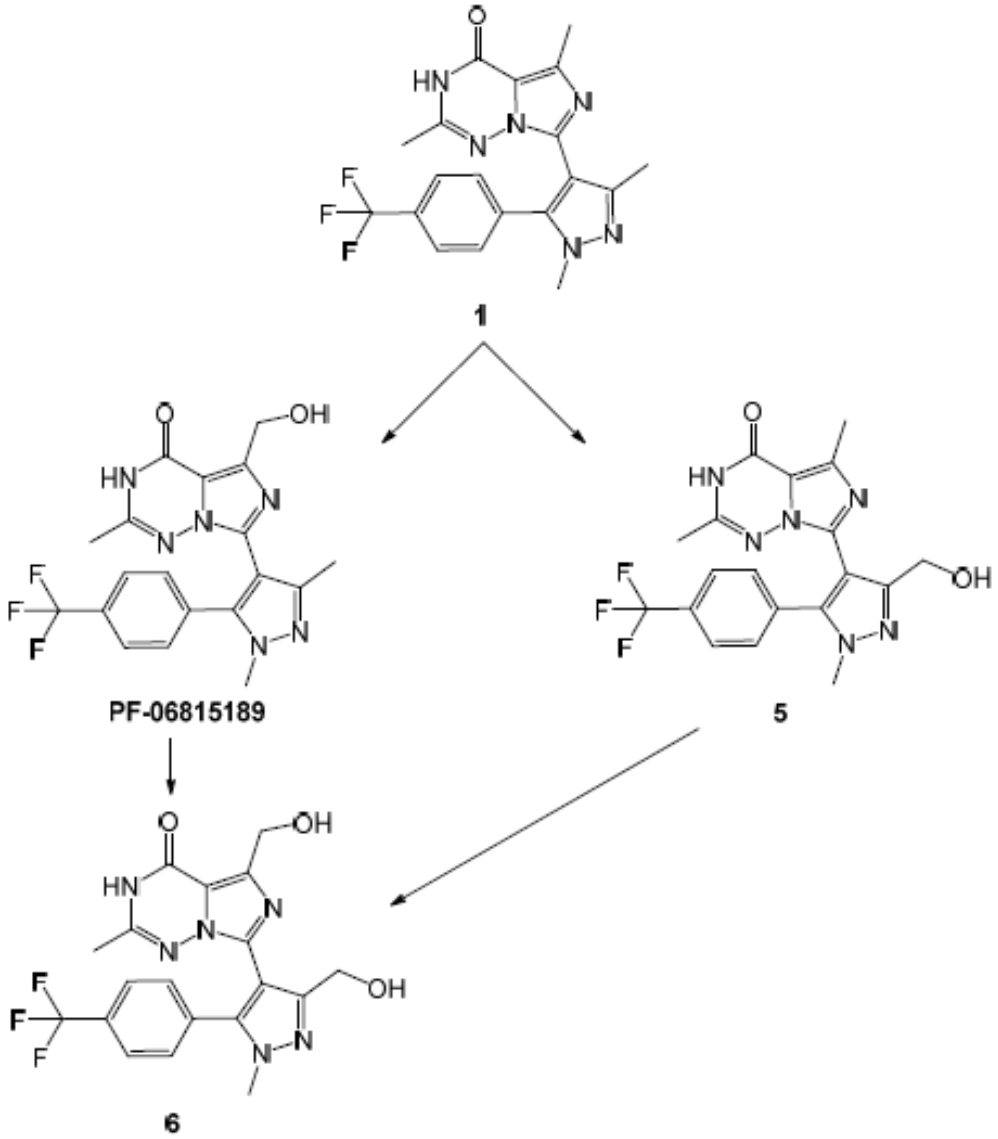

Stepan et. al., *ACS Med. Chem. Lett.* 2018, 9, 68−72

In Vitro PDE2 Potency and Absorption, Distribution, Metabolism, and Excretion (ADME) Characteristics of Analogues Obtained through C–H Oxidation

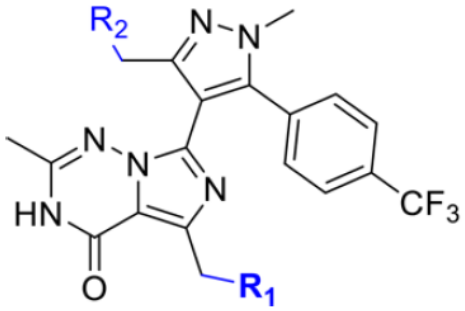

2 (PF-06815189): R_1 = OH, R_2 = H
5: R_1 = H, R_2 = OH
6: R_1 = R_2 = OH

	2	5	6
clogP/TPSA[a]	2.0/101	2.0/101	0.7/121
PDE2 IC_{50} (nM)[b]	0.4 (5)	6.9 (4)	7.8 (4)
HLM/HHEP $CL_{int,s}$[c] (mL/min/kg)	<8.0/<0.36	<8.0/–	<9.2/–
RRCK P_{app}[d] ($\times 10^{-6}$ cm/s)	8	17	5

[a]Topological polar surface area. [b]Number of replicates in parentheses. [c]Intrinsic scaled clearance. [d]Apparent passive permeability in the Ralph Russ Canine Kidney cell line.[19]

Stepan et. al., *ACS Med. Chem. Lett.* 2018, 9, 68–72

Synthesis of 1 and Biocatalytic Oxidation to 2

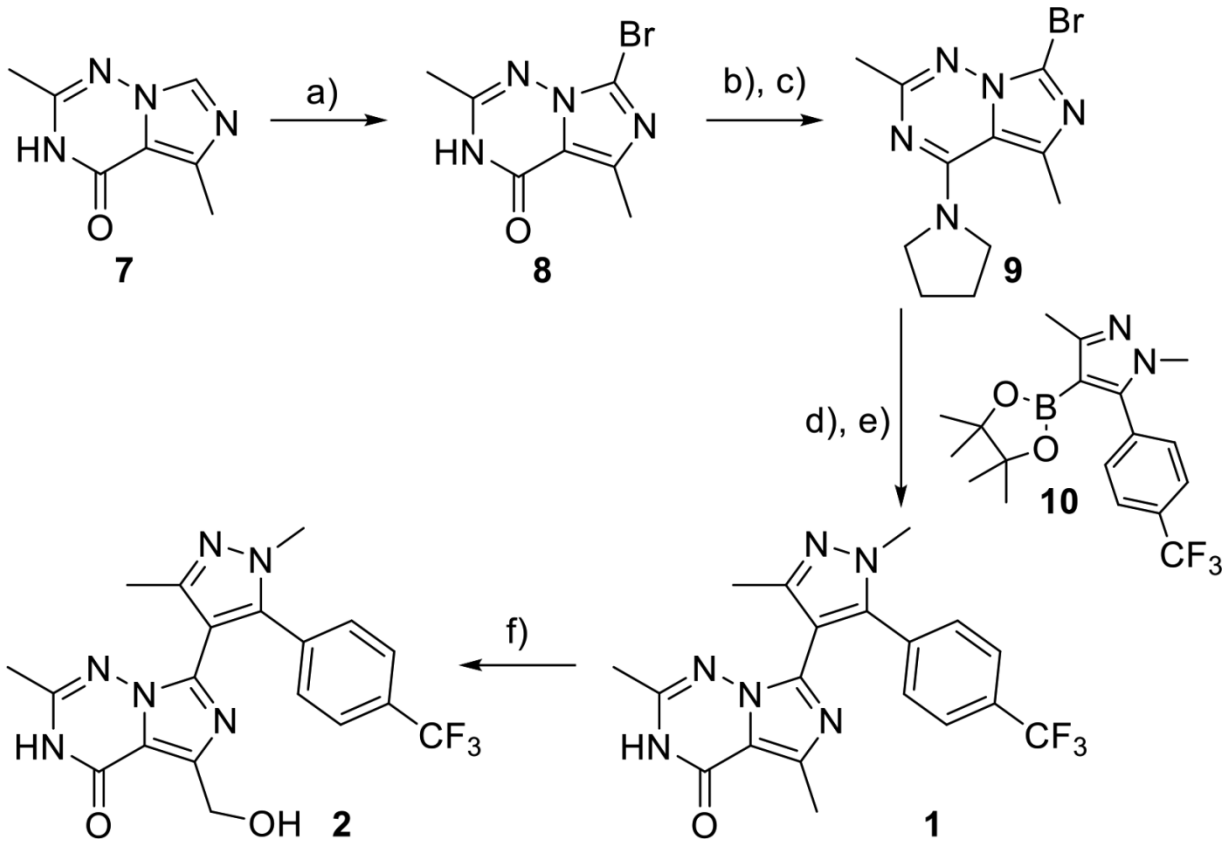

Reagents and conditions: (a) Br_2, DMF, 0–25 °C, 65%; (b) $POCl_3$, NEt_3, toluene, reflux; (c) pyrrolidine, NEt_3, CH_2Cl_2, 0–25 °C, 77%, two steps; (d) $Pd(dppf)Cl_2 \cdot CH_2Cl_2$, Na2CO3, dioxane/$H_2O$, 110 °C, 62%; (e) 1 M HCl, THF, reflux, 86%; (f) S. aerocolonigenes ATCC 39243 in Iowa medium, DMSO, 30 °C, 7 days, 20%.

Stepan et. al., *ACS Med. Chem. Lett.* 2018, 9, 68–72

SYNTHESIS OF CANDIDTATE 2

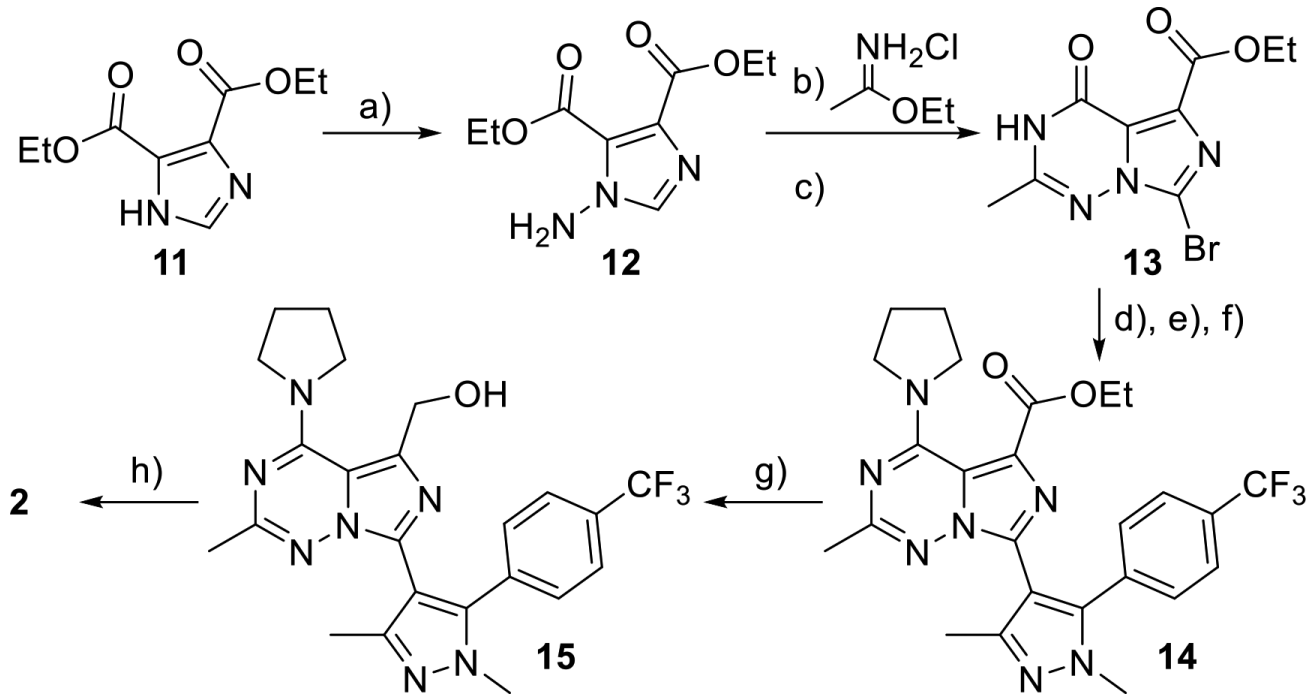

Reagents and conditions: (a) K2CO3, H2O/EtOH, H2NOSO3H, 0−25 °C, 78%; (b) DIPEA, 2-Me-THF, reflux; (c) NBS, HOAc/MeCN, 70 °C, 48%, 2 steps; (d) 1,2,4-triazole, POCl3, NEt3, CH2Cl2; (e) pyrrolidine, NEt3, CH2Cl2, 25 °C, 86%, 2 steps; (f) 10, Pd(dppf)Cl2·CH2Cl2, Na2CO3, dioxane/H2O, 110 °C, 91%; (g) LiBH4, THF, 50 °C, 98%; (h) 1 M HCl, THF, reflux, 92%.

Stepan et. al., *ACS Med. Chem. Lett.* 2018, 9, 68−72

IN-VIVO ACTIVITY

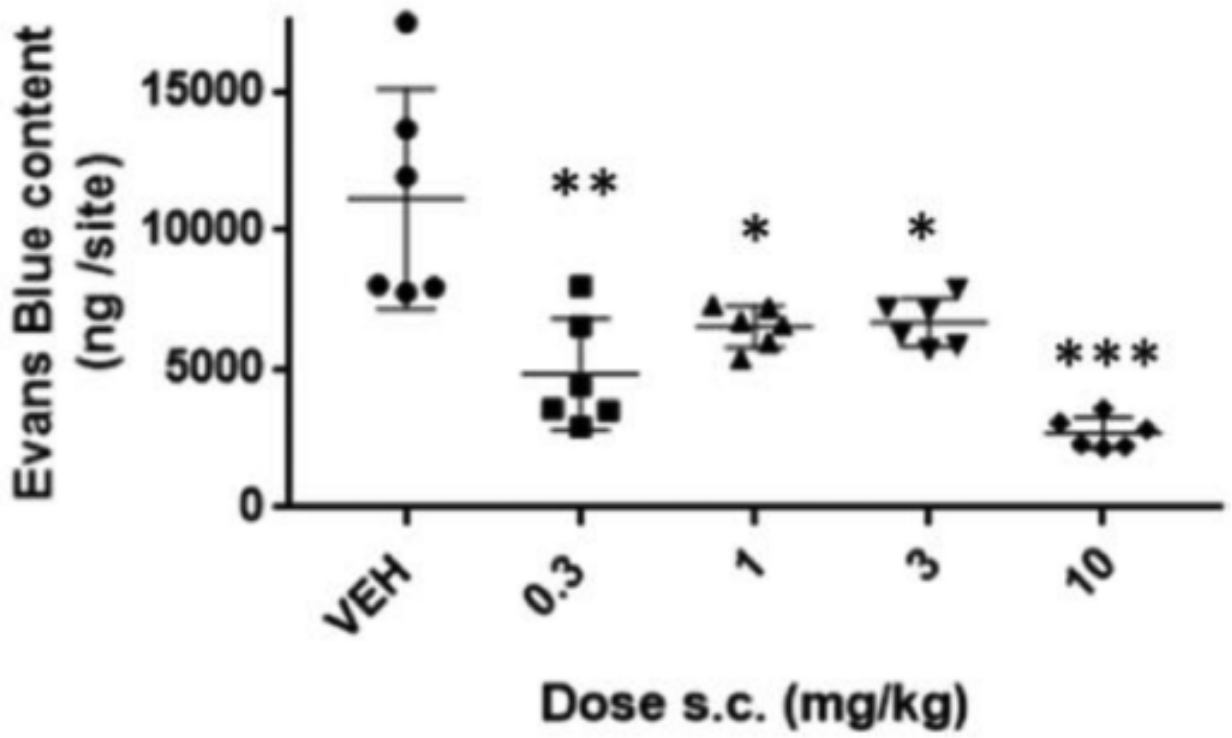

➢Administration of compound **2** significantly reduced histamine-induced extravasation of Evan's Blue dye in guinea pig skin (*p < 0.05, **p <0.01, ***p < 0.005).

Stepan et. al., *ACS Med. Chem. Lett.* 2018, 9, 68−72

Preclinical Pharmacokinetics of Compound 2

	CL_p[b] (mL/min/kg)	V_{ss}[c] (L/kg)	$t_{1/2}$[d] (h)	%F[e]	% renal clearance[f]
rat	28	1.5	1.2	50	22
dog	1.3	0.4	4.8	79	48
NHP	4.0	0.8	3.6	61	26

[a]N = 2 animals/dose in all studies. [b]Observed plasma clearance. [c]Steady-state volume of distribution. [d]Half-life. [e]Bioavailability. [f]Percent dose recovered in urine (0–24 h).

Stepan et. al., *ACS Med. Chem. Lett.* 2018, 9, 68−72

CONCLUSION

- Late-stage functionalization strategy using microsomal oxidation to the PDE2 inhibitor approach improved the drug-likeness of the early **lead 1** (LipE = 5.9 and LiMetE = 1.9) and allowed rapid identification of the potential clinical **candidate 2** (LipE = 7.4 and LipMetE =2.4)

- A daily dose of only 1.3 mg is required to achieve an average PDE2 IC_{90} coverage over 24 h, reflecting the exquisite drug-like attributes of 2

- Hydroxylation introduced the desired amount of renal clearance, minimizing the risk for clinical victim drug–drug interactions.

- Study highlights the impact of late-stage diversification technologies can have on drug discovery